Environmental Earth Sciences (2023) 82:388
https://doi.org/10.1007/s12665-023-11075-y

ORIGINAL ARTICLE

Thermal acoustic emission characteristics and damage evolution of granite under cyclic thermal shock

Honghao Yuan[1,2] · Qiang Sun[1,2] · Jishi Geng[1,2] · Liyun Tang[3] · Chao Lv[4] · Yuliang Zhang[5]

Received: 5 April 2023 / Accepted: 22 July 2023 / Published online: 2 August 2023

Abstract

In the process of geothermal energy extraction, the dry heat rock reservoir will be in the state of cyclic heating and water cooling for a long time. Therefore, it becomes important to study the effects of cyclic heating and cooling treatments on rock damage. In this context, the present study aimed to study the damage evolution process of rocks under cyclic thermal shock. In this paper, granite specimens were subjected to cyclic heating at the target temperatures of 200, 300, and 400 °C and cooling treatments using surface water spraying. The changes in the rock damage process during each heating cycle were monitored using the acoustic emission technique, and the damage mechanism and crack development mechanism of granite under cyclic thermal shock were discussed. The results show that granite will enter the rapid damage stage when it reaches a certain number of cycles (200℃, 300℃, 400℃ corresponds to the 16th, 8th, and 6th cycles, respectively) during the hot and cold cycling process the acoustic emission characteristics show a similar regularity: the inflection points a, b, c, and d appear near 40 °C, 150 °C, 240 °C, and 300 °C, respectively, when the acoustic emission signal becomes active and the cumulative ringing count increases rapidly, and the higher the heating temperature, the number of cycles when the granite enters the rapid damage stage and the temperature threshold for crack generation is advanced, when the heating temperature is 400 °C, the damage threshold point b and c is about 10 °C earlier than 300 °C. In addition, as the thermal cycle temperature and the number of cycles increased, the degree of damage to the rock intensified, and the width and density of the cracks on the surface of the granite also increased.

Keywords Granite · Thermal cycling · Acoustic emission · Cooling treatment

Introduction

Geothermal energy, as a clean renewable energy source, has good prospects for development because of its clean and widely distributed, renewable, and stable operation (Bahadori et al. 2013). In general, common dry heat rock (HDR) reservoirs consist of dense granite or other crystalline rocks at depths of about 5–6 km and temperatures between 150 and 500 °C (Zeng et al. 2013; Parvizi et al. 2017). Enhanced geothermal system (EGS) is an effective method to develop dry heat rock resources, which achieves heat recovery by injecting cold water into the target reservoir,

✉ Jishi Geng
gengjishi@cumt.edu.cn

Honghao Yuan
21209226123@stu.xust.edu.cn

Qiang Sun
sunqiang04@cumt.edu.cn

Liyun Tang
tangly@xust.edu.cn

Chao Lv
lyu.chao@xust.edu.cn

Yuliang Zhang
z_yl@tju.edu.cn

[1] College of Geology and Environment, Xi'an University of Science and Technology, Xi'an 710054, Shaanxi, China

[2] Geological Research Institute for Coal Green Mining, Xi'an University of Science and Technology, Xi'an 710054, China

[3] College of Architecture and Civil Engineering, Xi'an University of Science and Technology, Xi'an 710054, Shaanxi, China

[4] College of Energy Engineering, Xi'an University of Science and Technology, Xi'an 710054, Shaanxi, China

[5] School of Civil and Transportation Engineering, Hebei University of Technology, Tianjin 300401, China

where the cold-water flow in the rock fractures will absorb the heat energy in the target reservoir and convert the liquid water into steam for discharge (Poletto et al.2018; Zhang et al. 2020). In the process of geothermal energy extraction, the HDR reservoir rocks will be cyclically heated and cooled for a long time, so it is important to study the thermal damage of rocks under cyclic heating–cooling conditions for geothermal energy extraction engineering applications.

With the development of underground space and geothermal resources, many scholars have extensively studied the changes in macroscopic mechanical and physical properties of rocks under high-temperature cycling and thermal shock (David et al. 1999; Yavuz et al. 2011; Gautam et al. 2015; Sun et al. 2015; Wang et al. 2016; Kant et al. 2017; Kumari et al. 2019; Daoud et al. 2020; Lan et al. 2019, 2022; Shi et al. 2022, 2023). Thermal stresses caused by mineral expansion under high temperatures can lead to thermal cracking within the rock bedrock, and the resulting thermogenic cracks can impede heat transfer in the rock layer, increase porosity and permeability, and degrade the mechanical properties of the rock (Chaki et al. 2008; Gautam et al. 2016; Fan et al. 2017), In addition, static elastic modulus, and crack damage threshold of granite reached the highest when the heating temperature reached 300 °C (Yang et al. 2017). And thermal cycling and cooling rate can significantly affect the microcrack evolution, permeability, and fracture resistance of granite (Feng et al. 2020). Liu et al. (2019), Villarraga et al. (2018), and Gautam et al. (2020) investigated the effect of thermal cycling effect on the physical and mechanical properties of red sandstone, limestone, and granite, respectively, and the results showed that the increase in the number of thermal cycles led to strain accumulation, increase in porosity and permeability, and decrease in P-wave velocity, elastic modulus, and rock strength. In addition, Shen et al. (2021) studied the effect of different cooling shock treatments on high-temperature granites and found that the local distribution characteristics of macroscopic cracking became more pronounced as the refrigerant temperature decreased. Wang et al. (2020) investigated the effect of cooling on the fracture process of granite after high-speed heating and found that the effect of heating rate on the strength of granite was relatively small, and thermogenic microcracking had a significant effect on the strength reduction and mechanical properties of granite after heat treatment.

Acoustic emission (AE) technology can monitor the generation and expansion of microcracks during rock rupture in real time, which is based on the principle that when a rock is deformed or ruptured during the force, the strain energy is released in the form of elastic waves, and the acoustic emission parameters count the information of the whole process of rock damage and destruction, which can reflect the damage mechanism and damage nature of the rock (Geng et al. 2023; Ding et al. 2022; Peng et al. 2018; Liu et al. 2019; Sun et al. 2021). This technique is now widely used in the study of instability damage of rock-like materials. Yin et al. (2019) explored the damage pattern and microstructural changes of granite under cyclic heating and cooling treatments through acoustic emission events. Tschegg (2016) monitored the damage process in marble under thermal cycling by acoustic emission technique and analyzed to assess the structural damage in the rock. Daoud et al. (2020) showed that there is a temperature memory effect on the acoustic emission results of rocks under the effect of multiple cold and hot cycles.

In summary, there are more previous studies on the effects of high-temperature cycling and thermal shock on the physical and mechanical properties of rocks, but there are fewer studies on the damage evolution of rocks under cyclic thermal shock. In this paper, the thermal damage evolution of granite with different heating temperatures under the conditions of cyclic heating and water-cooling treatment is investigated using acoustic emission technique, which can help us to analyze the thermal damage mechanism and crack development mechanism of rocks under cyclic thermal shock more deeply.

Materials and methods

Samples

The granite specimens from Linyi City, Shandong Province, with good petrographic homogeneity and no obvious defects and fractures were selected for this test. X-ray diffraction analysis showed that the alkali feldspar and plagioclase composition content was 58.4%, quartz composition was 32.0%, amphibole content was 6.1% and mica content was 3.4%. And the specimen is processed into a cylindrical specimen of 50 mm in diameter and 25 mm in height.

Experimental equipment

The heating equipment selected for this experiment was a muffle furnace (SDTGA200, Hunan Shazhou Technology Co., Ltd.). The maximum heating temperature is 1000 °C, the temperature control accuracy is ± 2.5 °C, the maximum heating rate is 100 °C/min, and the maximum power is 3.5 kW. The DS5-8B full information acoustic emission signal analyzer manufactured by Softland Time Co., Ltd. in Beijing, China, was selected for the acoustic emission test, with 8 independent channels, each with a sampling speed of 3 M, and its continuous data throughput rate of 65.5 MB/s and waveform data throughput rate of 48 MB/s.

Experimental methods

Heating treatment

The granite samples were placed in a muffle furnace, and the acoustic emission signal probe was connected to it through a waveguide with the threshold set to 40 dB, and heated to 200 °C, 300 °C and 400 °C at a uniform rate of 4 °C/min, respectively. After the samples were heated to the target temperature, they were kept at a constant temperature in the furnace for 1 h to ensure uniform heating of the samples.

Cooling treatment

After 1 h of constant temperature exposure, the rock samples were removed from the furnace immediately and allowed to cool by spraying water on the surface (25 °C) every 40 s.

Circulation heating

In this experiment, the granite is treated with heating–cooling–heating cycle (Fig. 1). A total of 20, 20, 12, 5, and 5 cycles were performed for the 200 °C, 300 °C, 400 °C, 500 °C, and 600 °C groups of specimens, respectively.

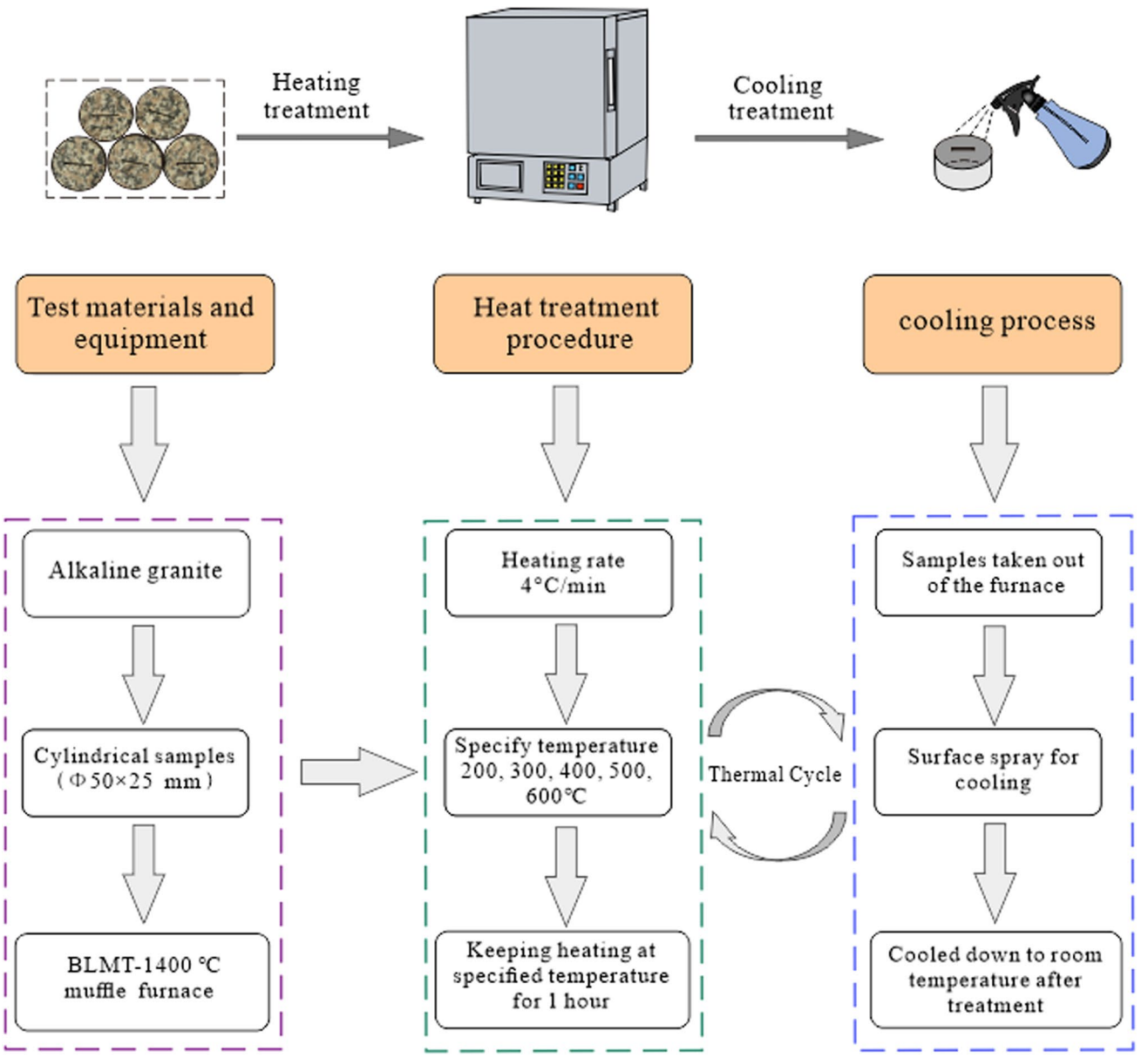

Fig. 1 Flow chart of the cycle

Meanwhile, the damage caused to the granite during the heating and cooling cycles was monitored using the acoustic emission technique.

Experimental results

Acoustic emission characteristics of granite during the cyclic heating

In this experiment, the granite heating and cooling process was monitored in real-time using acoustic emission equipment. And the number of cycles with more typical acoustic emission characteristics was screened at each thermal cycle temperature, based on which the process was divided into three stages according to the determined characteristics: a steady increase period, a calm period, and a steep increase period (Table 1). The acoustic emission characteristics of the steady increase period included an active acoustic emission signal, a steady increase in the cumulative ringing count, and a smooth cumulative ringing count curve.

The steep increase period was characterized by intensive or sporadic larger-valued ringing counts of the acoustic emission signal, rapid growth of cumulative ringing counts and a significant rise in the cumulative ringing count curve. The calm period was characterized by a lower acoustic emission signal, quiet cumulative ringing count, and less fluctuation in the cumulative ringing count curve.

As illustrated in Fig. 2, when the target heating temperature was 200 °C, the acoustic emission signal was low in the 1st–6th cycles, while the cumulative ringing count increased gradually. In the 7th cycle, the acoustic emission signal increased steeply as the temperature reached 75 °C, while the accumulated ringing count exhibited an intensive and rapid growth, demonstrating the phenomenon of thermal fatigue. In the 16–20 cycles, the acoustic emission characteristics behaved similarly, with an inflection point a near 40 °C, where the acoustic emission signal appeared and behaved intensively, and the cumulative ringing count increased from point a, then leveled off and started to rise again at point b.

As depicted in Fig. 3, when the target heating temperature was 300 °C in the first cycle, the acoustic emission signal increased rapidly after 170 °C, beyond which a steady increase followed by a steep increase was observed. In the 5th cycle, steep increases were observed at several time

Table 1 Stages of the cyclic heating and cooling process of granite based on the acoustic emission characteristics

Temperature	Cycles	Acoustic emission Characteristics		
		Steady growth period	Calm period	Steep increase period
200 °C	1	50–70 °C	70–150 °C	150–190 °C
	7	50–80 °C	–	80–190 °C
	11	60–80 °C 90–100 °C	60–90 °C 100–130 °C	130–190 °C
	16	30–90 °C 150–190 °C	90–150 °C	–
300 °C	1	170–220 °C	80–170 °C 200–260 °C	260–290 °C
	5	250–290 °C	60–100 °C 110–150 °C 170–250 °C	50 °C 100–110 °C 150–170 °C
	8	40–100 °C 150–210 °C 240–290 °C	100–150 °C 210–240 °C	—
	20	40–100 °C 150–210 °C 240–290 °C	100–150 °C 210–240 °C	—
400 °C	1	60–80 °C 170–230 °C	80–170 °C	230–390 °C
	5	–	100–160 °C 240–370 °C	50–100 °C 170–240 °C 370–390 °C
	6	30–80 °C 140–190 °C 220–390 °C	80–140 °C 190–220 °C	–
	12	30–80 °C 130–190 °C 220–390 °C	80–130 °C 190–220 °C	–

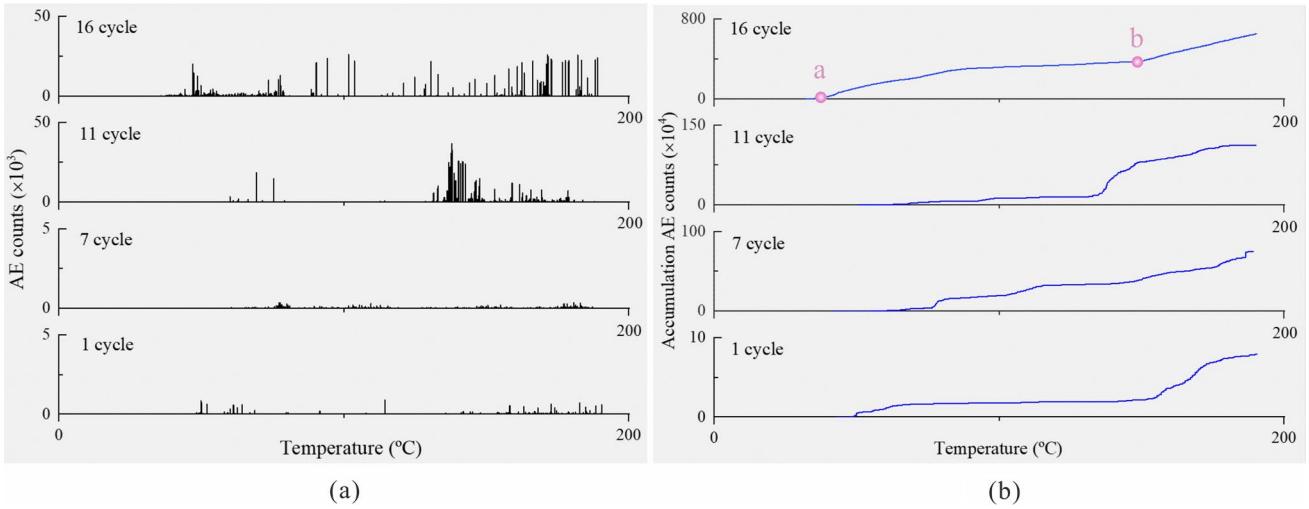

Fig. 2 The acoustic emission counts and cumulative acoustic emission counts at different number of cycles at the heating temperature of 200 °C, **a** Variation of acoustic emission counts with different number of cycles. **b** Variation of cumulative acoustic emission counts with different number of cycles

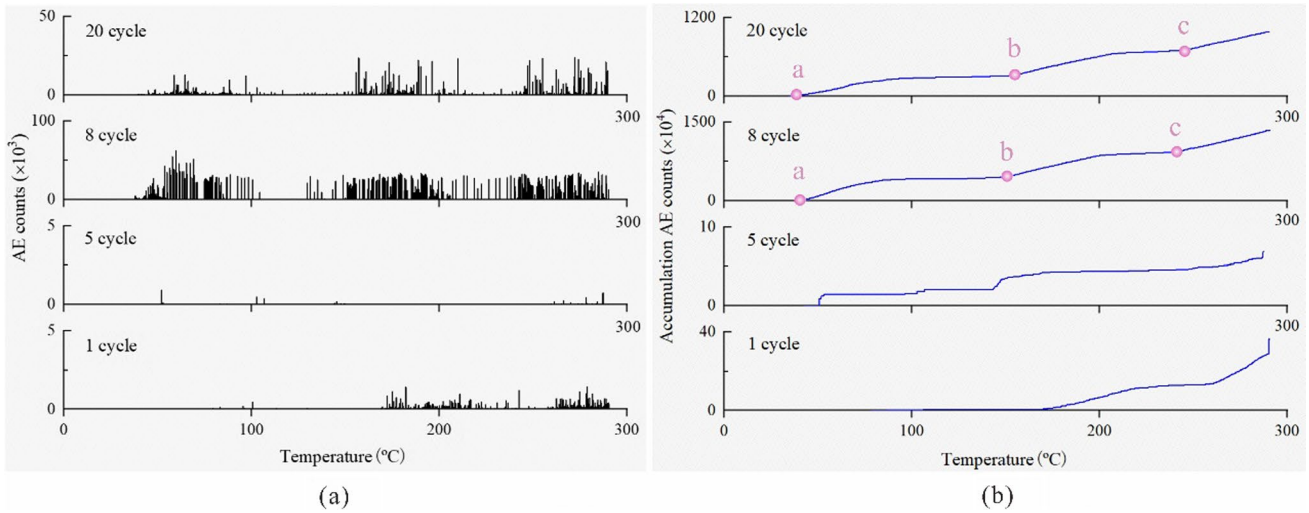

Fig. 3 The acoustic emission counts and cumulative acoustic emission counts at different number of cycles at the heating temperature of 300 °C, **a** Variation of acoustic emission counts with different number of cycles. **b** Variation of cumulative acoustic emission counts with different number of cycles

points. In 8–20 cycles, the acoustic emission characteristics behaved similarly, and the inflection point b appeared near 150 °C, the acoustic emission signal was active, the cumulative ringing count grew rapidly, and the cumulative ringing count curve showed a trend of first growth and then flattening in the ab and bc stages.

As depicted in Fig. 4, when the target heating temperature was 400 °C in the first cycle, the acoustic emission began increasing steadily at 60 °C. At 170 °C, large values of ringing counts appeared, and the acoustic emission signal began rising rapidly. In the 5th cycle, the acoustic emission signal exhibited several steep increases. In 6–12 cycles, the inflection point c appeared at about 240 °C, and the acoustic emission ringing count started to grow. The characteristics of acoustic emission signal in ab, bc, and cd stages were characterized by alternating steady increase period and calm period, and as the temperature increased, the steady increase period became longer and the calm period became shorter, and the acoustic emission signal became more and more active.

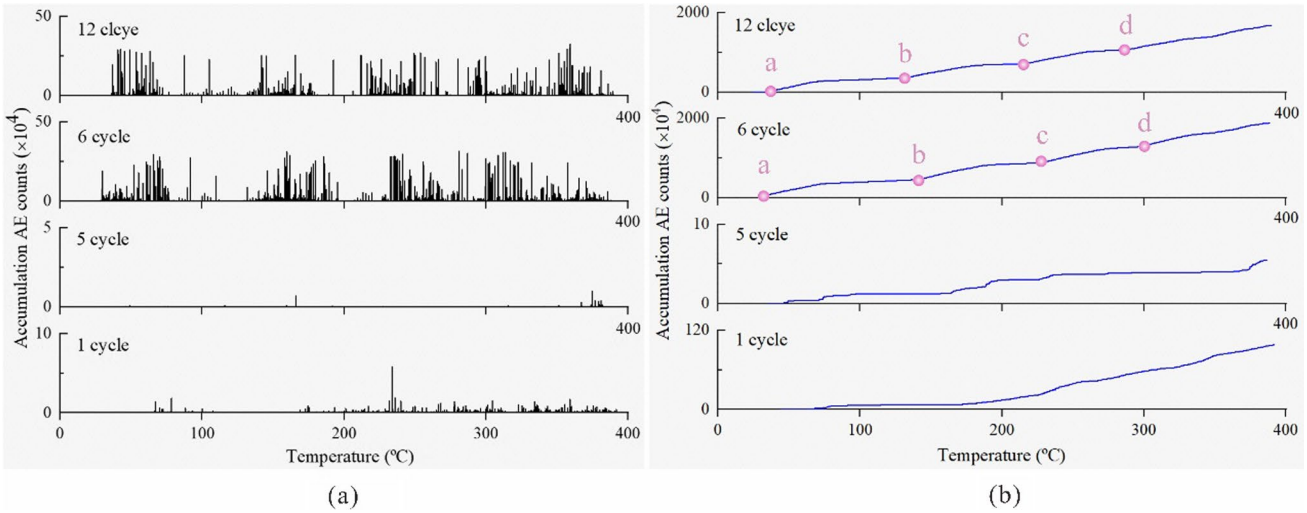

Fig. 4 The acoustic emission counts and cumulative acoustic emission counts at different number of cycles at the heating temperature of 400 °C, **a** Variation of acoustic emission counts with different number of cycles. **b** Variation of cumulative acoustic emission counts with different number of cycles

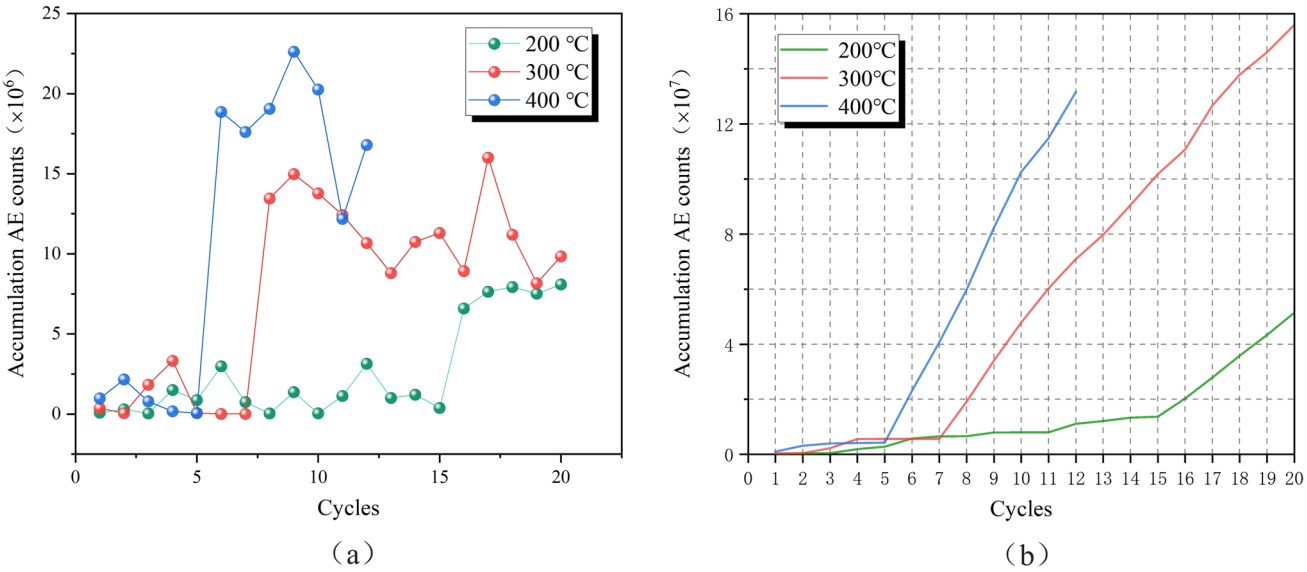

Fig. 5 **a** The cumulative acoustic emission counts at different number of cycles during the heating of granite. **b** The cumulative acoustic emission counts at different number of cycles during the heating of granite

Cumulative acoustic emission characteristics of granite during cyclic heating

Figure 5 shows the cumulative ringing counts of granite specimens during heating under hot and cold cycling conditions, In the first few cycles, the cumulative acoustic emission ringing count fluctuated less, and with the increase of the cycle number, the thermal damage accumulated continuously, when reaching a certain number of cycles (200, 300, 400 °C, respectively, in the 16th, 8th, 6th cycle), the granite entered a rapid damage stage, and its cumulative ringing count and cycle cumulative ringing count began to appear a significant increase, and the higher the heating temperature, the faster the rapid damage stage came.

Comparison of cracks prior to and after the cyclic heating process

Figure 6 shows the surface condition of granite after a certain number of cycles. At 200 °C, fewer cracks appeared

on the granite surface. As the number of cycles increased, the cracks became further evident. At 300 °C, the cracks appeared at the 5th cycle, and certain regions on the granite surface began peeling off at the 10th cycle, while at the 20th cycle, the crack regions of granite increased further and deepened, and the peeling regions also extended. At 400 °C, multiple cracks appeared at the 5th cycle, and the crack width and density increased gradually as the number of cycles increased further. According to the above findings, it was concluded that the damage caused to granite becomes increasingly severe as the heating temperature and the number of cycles increase.

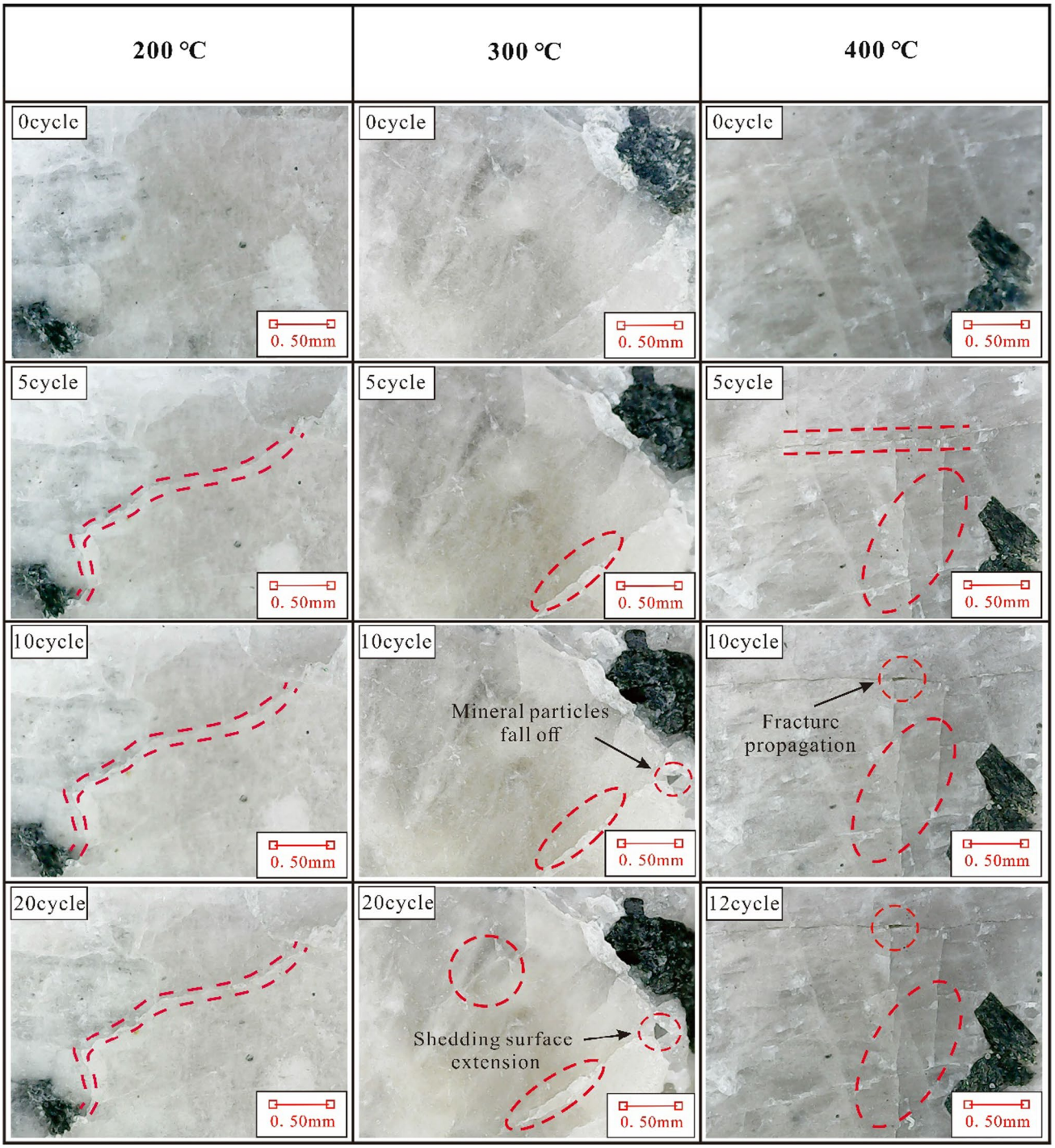

Fig. 6 Micrographs of granite after cold and hot cycles

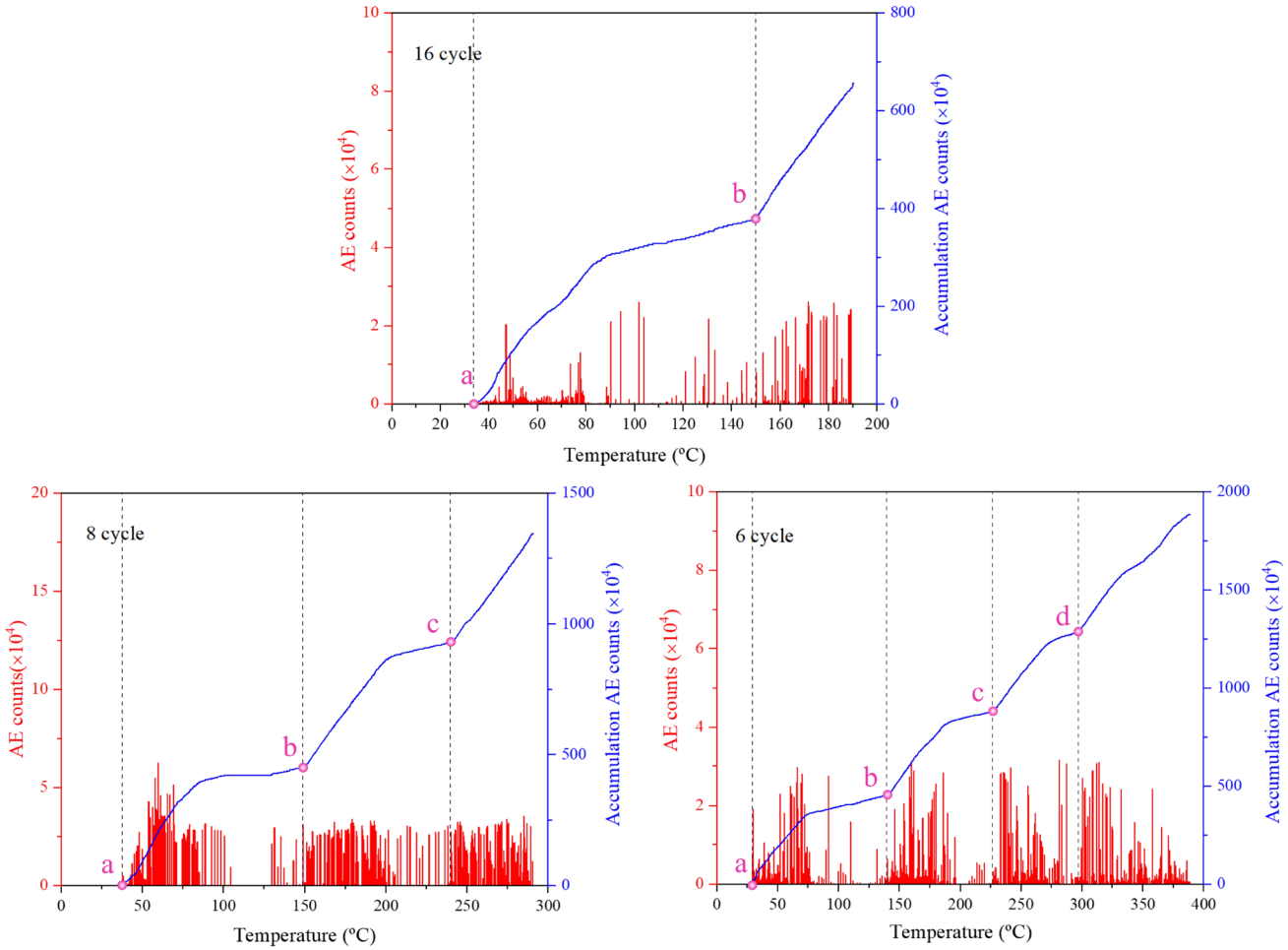

Fig. 7 Variation in the AE signal during cyclic heating at different target temperatures

Discussion and analysis

Thermoacoustic emission characteristic mode

In this experiment, the generation and expansion of cracks in granite during cyclic process were monitored in real time by acoustic emission technique. The output of the acoustic emission signal depends on the temperature level and the heating and water-cooling cycles. The acoustic emission activity is active throughout the heating process as the temperature increases or reaches a certain number of cycles. Figure 7 illustrates the variation in the acoustic emission (AE) phenomena at different cyclic heating temperatures after the granite specimen enters the rapid damage stage. Temperature close to 40 °C, acoustic emission signals appear and behave densely, which is due to the combination of cracks contracted during cooling treatment that start to expand under heating treatment and the start of escape of attached water; near 150 °C, acoustic emission signals are active and cumulative ringing counts increase rapidly, which is the temperature range for the loss of adsorbed water and weak interlayer bound water (Feng et al. 2020); near 240 °C, strongly bound water evaporates and escapes, and when the temperature reaches 300 °C, the crystalline water starts to evaporate and breaks free from the mineral lattice by 400 °C (Zhang et al. 2016; Hu et al. 2018; Gautam et al. 2019). The appearance of the inflection points a, b, c, and d in the acoustic emission signal signature during cyclic heating and the active degree exhibited by these points implies the continuous escape of free water, bound water, and water of crystallization from the granite, which increases the number of microcracks in the rock and generates many acoustic emission signals. With the escape and loss of moisture at each stage, the crack extension becomes relatively stable, and the acoustic emission signal gradually decreases. The overall characteristics of acoustic emission mainly demonstrate that when the granite specimen reaches a certain temperature threshold during the heating process, the acoustic emission signal begins to become active, the accumulated ringing

count begins growing rapidly, and ultimately tends to become calm. The steady increase period and the calm period appear alternately, and the calm period shortens gradually as the temperature rises. It was also observed that the inflection points a, b, and c gradually advance the temperature threshold for the occurrence of damage as the cycling temperature increases. In addition, it was observed that as the heat temperature of granite increased, the thermal damage it suffered during the cycle became more severe and the microcracks in the rock were more likely to generate and expand, and the temperature threshold at which thermal damage occurred at the inflection points a, b, and c was gradually advanced.

Damage mechanism of granite under cyclic heating and cooling conditions

The degree of damage to granite during the heating–water cooling cycle is mainly affected by four aspects: heating, water cooling, water-induced weakening, and thermal cycling. As depicted in Fig. 8, during the heating process, due to the significant differences in the thermal expansion coefficients of the different mineral particles in granite, uncoordinated deformation occurs between the particles, which generates thermal stresses. Once the thermal stresses exceed the ultimate strength between or within the minerals, microcracking occurs (Yang et al. 2017; Wu et al. 2021). In the subsequent cooling stage, water could intrude into the rock body through micropores and microfractures, which would further weaken the bond strength between the mineral grains and exacerbate the propagation and development of microcracks (Kumari et al. 2017; Li et al. 2021).

Moreover, this water-induced weakening is one of the factors leading to rock deterioration, with this weakening effect being further pronounced in the rocks with thermogenic cracking beyond high temperatures, particularly the rocks containing water-sensitive minerals, such as mica and montmorillonite (Zhang et al. 2021). The silica component contained in granite loses its structural stability easily due to the hydrolysis of silicon (Fig. 9) (Zhou et al. 2018) according to the following reaction:

$$(-\text{Si-O-Si-}) + (\text{H-O-H}) \rightleftharpoons (\text{-Si-OH-HO-Si-}).$$

Under cyclic action, rocks are subjected to alternating stresses arising from inhomogeneous expansion and contraction of minerals, which results in fatigue damage caused to the rocks and could lead to the generation and extension of microcracks even if the stresses are much less than the ultimate strength (Cai et al. 2019; Zhang et al. 2021). In addition, granite is mainly composed of quartz, which plays an important role in determining the physical properties of the rock (Gautam et al. 2019), and Yin et al. (2021) found by X-ray diffraction technique (XRD) that the maximum diffraction intensity of quartz decreased by 25.82–38.89% and 13.42–31.93% with increasing temperature and number of cycles, respectively, and microthermal defects gradually developed, leading to a weakening of the macroscopic load-bearing capacity. The uneven thermal expansion and cooling contraction cycles, the evaporative escape of mineral-bound water, and the decomposition and melting of the mineral components result in the gradual formation of rock micro-defects and the accumulation of thermal damage (Yin et al. 2021). As the number of cycles increases, the micro-defects

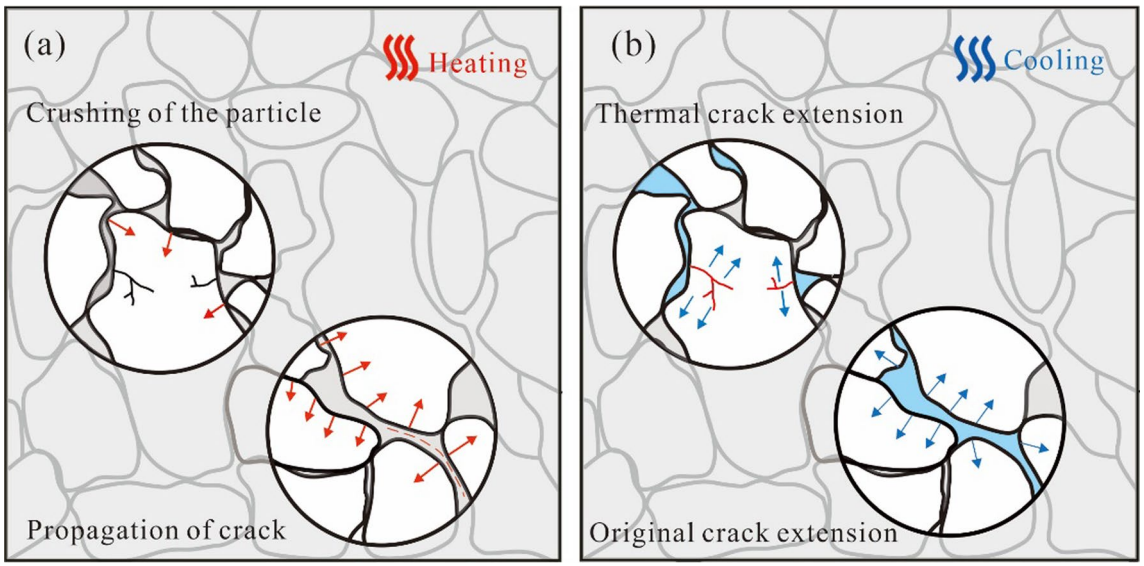

Fig. 8 Generation of microcracks in granite under cyclic heating and cooling conditions

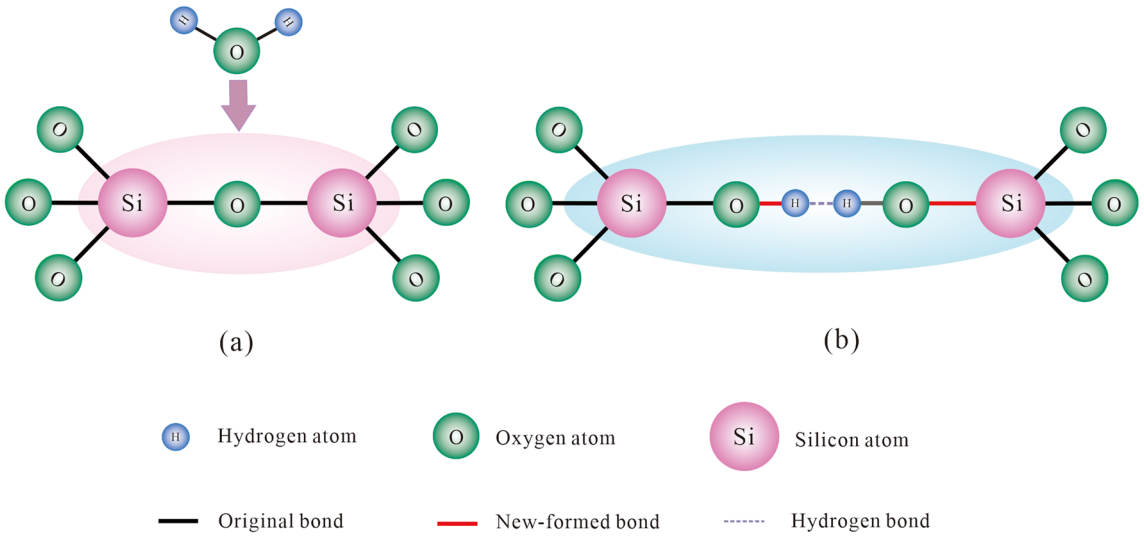

Fig. 9 Schematic diagram of the hydrolysis of silicon dioxide. **a** A silicon dioxide molecule (SiO_2) with a strong Si–O–Si bond encounters a water molecule (H_2O). **b** After hydrolysis, the strong Si–O–Si bond is replaced with a hydrogen bond

within the rock extend, providing enough deformation space for mineral expansion, thus reducing the thermal stress effect between mineral particles and stabilizes the degradation gradually (Rong et al. 2021). Consequently, when the thermal cycle reaches a certain number, the acoustic emission characteristics of the heating process remain almost constant (16, 8, and 6 cycles corresponded to 200, 300, and 400 °C, respectively, in the present study).

Cyclic cracking analysis

Due to the difference in the coefficient of thermal expansion of different mineral grains, which leads to thermal stresses caused by the mutual constraint between mineral grains during heating, resulting in thermogenic cracking in granite. In the cooling process, the cooling treatment with surface water injection caused a rapid temperature drop in the high-temperature granite and a sharp contraction of its mineral grains, while the core region of the rock remained unaffected by the cooling impact and was in a state of high-temperature expansion. The large temperature gradient between these two regions resulted in the formation of tangential tensile stresses on the surface of the rock (Rathnaweera et al. 2018). In separate studies, Kim et al. (2013) and Nasseri et al. (2009) indicated that intergranular compression and tensile forces cause thermal cracking in granite during the heating and cooling cycle when these forces exceed the local strength. In addition, Shi et al. (2020) showed that the length and width of microcracks within the rock and the number of microcracks increase in number with the number of thermal cycles. The damage of the specimens in this paper under the cycle is shown in Figs. 7 and 8, from which it can be seen that with the increase of the thermal cycle temperature and the increase of the number of times, the thermal damage of the rock is gradually serious, and the width and density of the crack area on the surface of granite also increase.

Conclusion

To obtain insights into the evolution of thermal damage in rocks under cyclic heating and cooling conditions during geothermal energy extraction, the acoustic emission characteristics of different thermal cycle temperature granite in the process of circulation heating and water cooling were analyzed. In addition, the damage mechanism and the crack expansion law of granite were studied. The main findings were as follows.

In the thermal cycling process, when reaching a certain number of cycles (200 °C, 300 °C, and 400 °C, corresponding to the 16, 8, and 6 cycles), granite entered the rapid damage stage, the acoustic emission characteristics exhibited a similar pattern, and the cycle cumulative ringing count of granite increased significantly. The acoustic emission characteristics show a similar regularity: the inflection points a, b, c, and d appear near 40 °C, 150 °C, 240 °C, and 300 °C, respectively, when the acoustic emission signal becomes active and the cumulative ringing count increases rapidly, and the higher the heating temperature, the number of cycles to enter the rapid damage stage and the temperature threshold for cracking in granite will earlier, when the heating temperature is 400 °C,

the damage threshold point b and c is about 10 °C earlier than 300 °C.

During the thermal cycle, along with the continuous escape of free water, bound water, and crystalline water in the granite, the number of microcracks in the rock increases and the acoustic emission signal grows rapidly, and with the escape and loss of water at each stage, the crack expansion becomes relatively stable and the acoustic emission signal gradually decreases, and the overall characteristics show that the steady increase period alternates with the calm period.

In the thermal cycling process, as the temperature of the thermal cycle rises and the number of cycles increases, the degree of damage caused to the rock becomes increasingly severe, and the width and density of the cracks generated on the surface of granite also increase.

Acknowledgements This research was supported by the National Natural Science Foundation of China (Grant no. 41972288).

Author contributions The contribution of authors in the production of the journal article, titled "Thermal acoustic emission characteristics and damage evolution of granite under cyclic thermal shock" as below. Honghao Yuan: Experimental Data Processing, Methodology, First Draft; Qiang Sun: Responsible for supervising writing and experiments and providing methodologies; Jishi Geng: Sample preparation, acoustic emission test participants; Liyun Tang: Data collation and analysis; Chao Lv: Main participants of the field test; Yuliang Zhang: .Technical guidance on test methods.

Data availability Not applicable.

Declarations

Conflict of interest The authors declare that they have no known competing financial interests or personal relationships that could have appeared to influence the work reported in this paper.

References

Bahadori A, Zendehboudi S, Zahedi G (2013) A review of geothermal energy resources in Australia: current status and prospects. Renew Sustain Energy Rev 21:29–34. https://doi.org/10.1016/j.rser.2012.12.020

Cai X, Zhou Z, Liu K, Du X, Zhang H (2019) Water-weakening effects on the mechanical behavior of different rock types: phenomena and mechanisms. Appl Sci. https://doi.org/10.3390/app9204450

Chaki S, Takarli M, Agbodjan WP (2008) Influence of thermal damage on physical properties of a granite rock: porosity, permeability and ultrasonic wave evolutions. Constr Build Mater 22:1456–1461. https://doi.org/10.1016/j.conbuildmat.2007.04.002

Daoud A, Browning J, Meredith PG, Mitchell TM (2020) Microstructural controls on thermal crack damage and the presence of a temperature-memory effect during cyclic thermal stressing of rocks. Geophys Res Lett. https://doi.org/10.1029/2020GL088693

David C, Menéndez B, Darot M (1999) Influence of stress-induced and thermal cracking on physical properties and microstructure of la peyratte granite. Int J Rock Mech Min Sci 36(4):433–448. https://doi.org/10.1016/S0148-9062(99)00010-8

Ding ZW, Li XF, Huang X et al (2022) Feature extraction, recognition, and classification of acoustic emission waveform signal of coal rock sample under uniaxial compression. Int J Rock Mech Min Sci 160:105262. https://doi.org/10.1016/j.ijrmms.2022.105262

Fan LF, Wu ZJ, Wan Z, Gao JW (2017) Experimental investigation of thermal effects on dynamic behavior of granite. Appl Therm Eng 125:94–103. https://doi.org/10.1016/j.applthermaleng.2017.07.007

Feng G, Wang X, Wang M, Kang Y (2020) Experimental investigation of thermal cycling effect on fracture characteristics of granite in a geothermal-energy reservoir. Eng Fract Mech 235:107180

Gautam PK, Verma AK, Maheshwar S, Singh TN (2015) Thermo-mechanical analysis of different types of sandstone at elevated temperature. Rock Mech Rock Eng. https://doi.org/10.1007/s00603-015-0797-8

Gautam PK, Verma AK, Jha MK, Sarkar K, Singh TN, Bajpai RK (2016) Study of strain rate and thermal damage of Dholpur sandstone at elevated temperature. Rock Mech Rock Eng 49(9):3805–3815. https://doi.org/10.1007/s00603-016-0965-5

Gautam PK, Verma AK, Jha MK, Sharma P, Singh TN (2018) Effect of high temperature on physical and mechanical properties of jalore granite. J Appl Geophys. https://doi.org/10.1016/j.jappgeo.2018.07.018

Gautam PK, Verma AK, Singh TN, Hu W, Singh KH (2019) Experimental investigations on the thermal properties of jalore granitic rocks for nuclear waste repository. Thermochim Acta 681:178381. https://doi.org/10.1016/j.tca.2019.178381

Gautam PK, Dwivedi R, Kumar A, Kumar A, Singh TN (2020) Damage characteristics of jalore granitic rocks after thermal cycling effect for nuclear waste repository. Rock Mech Rock Eng 9:1–20. https://doi.org/10.1007/s00603-020-02260-7

Geng JS, Sun Q, Li H, Yang YR (2023) Deterioration of mudstone exposed to cyclic hygrothermal conditions based on thermoacoustic emission. Constr Build Mater 386:131581

Hu J, Sun Q, Pan X (2018) Variation of mechanical properties of granite after high-temperature treatment. Arab J Geosci 11(2):43. https://doi.org/10.1007/s12517-018-3395-8

Kant MA, Ammann J, Rossi E et al (2017) Thermal properties of Central Aare granite for temperatures up to 500 °C: irreversible changes due to thermal crack formation. Geophys Res Lett 44(2):771–776. https://doi.org/10.1002/2016GL070990

Kim K, Kemeny J, Nickerson M (2013) Effect of rapid thermal cooling on mechanical rock properties. Rock Mech Rock Eng 47(6):2005–2019. https://doi.org/10.1007/s00603-013-0523-3

Kumari WGP, Ranjith PG, Perera MSA, Shao S, Chen BK, Lashin A (2017) Mechanical behaviour of Australian strathbogie granite under in-situ stress and temperature conditions: an application to geothermal energy extraction. Geothermics 65(Jan.):44–59. https://doi.org/10.1016/j.geothermics.2016.07.002

Kumari W, Beaumont DM, Ranjith PG, Perera M, AvanthiIsaka BL, Khandelwal M (2019) An experimental study on tensile characteristics of granite rocks exposed to different high-temperature treatments. Geomech Geophys Geo Energy Geo Resour. https://doi.org/10.1007/s40948-018-0098-2

Lan H, Chen J, Macciotta R (2019) Universal confined tensile strength of intact rock open. Sci Rep. https://doi.org/10.1038/s41598-019-42698-6

Lan H, Zhang Y, Macciotta R, Li L, Wu Y, Bao H (2022) The role of discontinuities in the susceptibility, development, and runout of rock avalanches: a review. Landslides 6:19. https://doi.org/10.1007/s10346-022-01868-w

Li ZW, Zhang YJ, Gong YH, Zhu GQ (2020) Influences of mechanical damage and water saturation on the distributed thermal

conductivity of granite. Geothermics 83:101736. https://doi.org/10.1016/j.geothermics.2019.101736
Li Q, Li X, Yin T (2021) Factors affecting pore structure of granite under cyclic heating and cooling: a nuclear magnetic resonance investigation. Geothermics 96(4):102198. https://doi.org/10.1016/j.geothermics.2021.102198
Liu Q, Qian Z, Wu Z (2019) Micro/macro physical and mechanical variation of red sandstone subjected to cyclic heating and cooling: an experimental study. Bull Eng Geol Env. https://doi.org/10.1007/s10064-017-1196-z
Nasseri MHB, Tatone BSA, Grasselli G, Young RP (2009) Fracture toughness and fracture roughness interrelationship in thermally treated westerly granite. Pure Appl Geophys 166(5–7):801–882. https://doi.org/10.1016/j.ijrmms.2006.09.008
Parvizi H, Rezaei-Gomari S, Nabhani F (2017) Robust and flexible hydrocarbon production forecasting considering the heterogeneity impact for hydraulically fractured wells. Energy Fuels 31:8481–8488. https://doi.org/10.1021/acs.energyfuels.7b00738
Peng J, Guan R, Ming C, Yao MD, Zhou CB (2016) Physical and mechanical behaviors of a thermal-damaged coarse marble under uniaxial compression. Eng Geol 200(12):88–93. https://doi.org/10.1016/j.enggeo.2015.12.011
Poletto F, Farina B, Carcione JM (2018) Sensitivity of seismic properties to temperature variations in a geothermal reservoir. Geothermics 76(4):149–163. https://doi.org/10.1016/j.geothermics.2018.07.001
Rathnaweera TD, Ranjith PG, Gu X, Perera M, Kumari W, Wanniarachchi W et al (2018) Experimental investigation of thermomechanical behaviour of clay-rich sandstone at extreme temperatures followed by cooling treatments. Int J Rock Mech Min Resourc 107:208–223. https://doi.org/10.1016/j.ijrmms.2018.04.048
Rong G, Sha S, Li B, Chen Z, Zhang Z (2021) Experimental investigation on physical and mechanical properties of granite subjected to cyclic heating and liquid nitrogen cooling. Rock Mech Rock Eng. https://doi.org/10.1007/s00603-021-02390-6
Shen Y, Yuan J, Hou X, Hao J, Bai Z, Li T (2021) The strength changes and failure modes of high-temperature granite subjected to cooling shocks. Geomech Geophys Geo-Energy Geo-Resour 7(1):1–18. https://doi.org/10.1007/s40948-020-00214-5
Shi X, Gao L, Wu J, Zhu C, Chen S, Zhuo X (2020) Effects of cyclic heating and water cooling on the physical characteristics of granite. Energies. https://doi.org/10.3390/en13092136
Shi Q, Cui S, Wang S, Mi Y, Sun Q, Wang S et al (2022) Experiment study on CO_2 adsorption performance of thermal treated coal: inspiration for CO_2 storage after underground coal thermal treatment. Energy 254:124392
Shi Q, Kou B, Wang S, Sun Q, Xue W, Ji R et al (2023) Porosity changes in thermally-treated bituminous coal during step-by-step crushing: implications for closed pore variations with temperature. Nat Resour Res 32(3):1339–1358. https://doi.org/10.1007/s11053-023-10194-4
Sun Q, Zhang W, Xue L, Zhang Z, Su T (2015) Thermal damage pattern and thresholds of granite. Environ Earth Sci 74(3):2341–2349. https://doi.org/10.1007/s12665-015-4234-9
Sun H, Ma L, Liu W, Spearing A, Han J, Fu Y (2021) The response mechanism of acoustic and thermal effect when stress causes rock damage. Appl Acoust. https://doi.org/10.1016/j.apacoust.2021.108093
Tschegg EK (2016) Environmental influences on damage and destruction of the structure of marble. Int J Rock Mech Min Sci 89(Complete):250–258. https://doi.org/10.1016/j.ijrmms.2016.09.006
Villarraga CJ, Casc-Barbier M, Vaunat J, Darrozes J (2018) The effect of thermal cycles on limestone mechanical degradation. Int J Rock Mech Min Sci 109:115–123. https://doi.org/10.1016/j.ijrmms.2018.06.017
Wang P, Xu J, Liu S, Wang H (2016) Dynamic mechanical properties and deterioration of red sandstone subjected to repeated thermal shocks. Eng Geol 212:44–52. https://doi.org/10.1016/j.enggeo.2016.07.015
Wang F, Konietzky H, Thomas F, Li Y, Dai Y (2019) Impact of cooling on fracturing process of granite after high-speed heating. Int J Rock Mech Min Sci. https://doi.org/10.1016/j.ijrmms.2019.104155
Wang J, Zuo J, Sun Y, Wen J (2020) The effects of thermal treatments on the fatigue crack growth of beishan granite: an in situ observation study. Bull Eng Geol Environ. https://doi.org/10.1007/s10064-020-01966-w
Wu Y, Li XZ, Huang Z, Wang YC, Deng LC (2021) Effect of thermal damage on tensile strength and microstructure of granite: a case study of Beishan, China. Geomech Geophys Geo-Energy Geo-Resour. https://doi.org/10.1007/s40948-021-00278-x
Yang S-Q, Ranjith PG, Jing H-W, Tian W-L, Ju Y (2017) An experimental investigation on thermal damage and failure mechanical behavior of granite after exposure to different high temperature treatments. Geothermics 65:180–197. https://doi.org/10.1016/j.geothermics.2016.09.008
Yavuz H (2011) Effect of freeze–thaw and thermal shock weathering on the physical and mechanical properties of an andesite stone. Bull Eng Geol Environ 70(2):187–192. https://doi.org/10.1007/s10064-010-0302-2
Yin T, Li Q, Li X (2019) Experimental investigation on mode i fracture characteristics of granite after cyclic heating and cooling treatments. Eng Fract Mech 222:106740. https://doi.org/10.1016/j.engfracmech.2019.106740
Yin Q, Wu J, Zhu C, Wang Q, Xie J (2021) The role of multiple heating and water cooling cycles on physical and mechanical responses of granite rocks. Geomech Geophys Geo-Energy Geo-Resourc. https://doi.org/10.1007/s40948-021-00267-0
Zeng YC, Su Z, Wu NY (2013) Numerical simulation of heat production potential from hot dry rock by water circulating through two horizontal wells at desert peak geothermal field. Energy 56:92–107. https://doi.org/10.1016/j.energy.2013.04.055
Zhang W, Sun Q, Hao S, Geng J, Lv C (2016) Experimental study on the variation of physical and mechanical properties of rock after high temperature treatment. Appl Therm Eng 98:1297–1304. https://doi.org/10.1016/j.applthermaleng.2016.01.010
Zhang Z, Ma B, Ranjith PG, Yang S, Zhou L (2020) Indications of risks in geothermal systems caused by changes in pore structure and mechanical properties of granite: an experimental study. Bull Eng Geol Environ 79(10):5399–5414. https://doi.org/10.1007/s10064-020-01901-z
Zhang B, Tian H, Dou B, Zheng J, Liu H (2021) Macroscopic and microscopic experimental research on granite properties after high-temperature and water-cooling cycles. Geothermics 93:102079. https://doi.org/10.1016/j.geothermics.2021.102079
Zhou Z, Cai X, Ma D, Cao W, Chen L, Zhou J (2018) Effects of water content on fracture and mechanical behavior of sandstone with a low clay mineral content. Eng Fract Mech 193:47–65. https://doi.org/10.1016/j.engfracmech.2018.02.028